

1 **Critical analyses of nitrous oxide emissions in a full scale activated sludge system**  
2 **treating low carbon-to-nitrogen ratio wastewater**

3 **M. Spinelli<sup>1</sup>, A.L. Eusebi<sup>1\*</sup>, V. Vasilaki<sup>2</sup>, E. Katsou<sup>2</sup>, N. Frison<sup>3</sup>, D.Cingolani<sup>1</sup>, F. Fatone<sup>1</sup>**

4  
5 <sup>1</sup> Dipartimento SIMAU, Facoltà di Ingegneria, Università Politecnica delle Marche, Via Brecce  
6 Bianche, 12, 60100 Ancona, IT. a.l.eusebi@univpm.it

7 <sup>2</sup> Department of Civil Engineering and Environmental Engineering; Institute of Environment, Health  
8 and Societies, Brunel University London, Uxbridge Campus, Middlesex, UB8 3PH, Uxbridge, UK.

9 <sup>3</sup> Department of Biotechnology, University of Verona, Strada Le Grazie 15, Verona, IT

**Abstract:** A critical analysis of nitrous oxide emissions in a full-scale modified Ludzack Ettinger plant treating municipal wastewater with low carbon to nitrogen ratio is presented. The results of N<sub>2</sub>O emissions were processed by coupling classical (liquid chemical/physical characterization) and new data analytics techniques (online gaseous emissions and statistical analysis). Correlation between the operational parameters of the plant and long-term online monitored nitrous oxide emissions was conducted. The analysis considered the effect of off-gas sampling methods, the variability of feeding characteristics and the main liquid process variables as the principle parameters that may affect nitrous oxide emissions. In order to detect and assess the causal relationships between online monitored system variables and nitrous oxide emissions, statistical and event-based sensitivity analysis was adopted to identify causal relationships between the variables of the system. Observations revealed that lower ratio between carbon and nitrogen (COD:N) resulted in higher N<sub>2</sub>O emissions. The average nitrous oxide emission factors changed from 0.0089 gN<sub>2</sub>O/kgTN<sub>in</sub> to 0.051 gN<sub>2</sub>O/kgTN<sub>in</sub>, that corresponded to denitrification limited by organic carbon availability. The nitrous oxide dynamics were not significantly influenced by dissolved oxygen variations (within the range of 1.5 – 2 mg/L). However daily peaks of nitrous oxide emissions occurred when aeration flow-rate resulting was higher and stripped more nitrous oxide from liquid.

**Keywords:** Nitrous oxide emissions, Full-scale monitoring, Activated sludge, Sensitivity analysis; Gas sampling assessment, Emission Factors

10

11

12

13

14

## 15 **1. Introduction**

16 Biological processes are significant sources of greenhouse gases (GHGs), mainly carbon dioxide  
17 (CO<sub>2</sub>), methane (CH<sub>4</sub>) and dinitrogen oxide (N<sub>2</sub>O) in wastewater treatment plants (WWTPs)  
18 (Kampschreur et al., 2008). N<sub>2</sub>O emissions are considered as the most potent (~300 more than CO<sub>2</sub>)  
19 contributor to global warming. Numerous studies to date have focussed on real-field N<sub>2</sub>O monitoring  
20 and the understanding of the causes on N<sub>2</sub>O formation (IPPC, 2013). Several studies reveal that  
21 characteristics of the wastewater, operating parameters, configuration, environmental conditions and  
22 microbiological diversity of the biological processes have significant impact on N<sub>2</sub>O generation and  
23 on operational carbon footprint of WWTPs. Critical effect was found in relation to the carbon to  
24 nitrogen ratio both in lab- or pilot- scale biofilm systems (He et al., 2017; Zhang et al., 2016), for  
25 aerobic granules and suspended activated sludge (Gao et al., 2016; Sun et al., 2014; He et al., 2017;  
26 Ge et al., 2017). Modelling studies also confirm the phenomena (Jose et al., 2016; Law et al., 2012).  
27 To the best of authors' knowledge the effect low C:N on N<sub>2</sub>O emissions in full scale WWTPs has not  
28 been studied. Moreover, there is little evidence of extensive analytical studies in the literature  
29 regarding GHGs emissions from full scale plants. Therefore, quantifying the N<sub>2</sub>O production and  
30 determining an effective mitigation approach to employ in existing full scale biological processes is  
31 needed.

32 Uncertainties and potential sources of error of the monitoring equipment (e.g. noise factors) and  
33 variability in the sampling chamber and technique can contribute to the lack of accurate and robust  
34 measurements of N<sub>2</sub>O (Desloover et al., 2016) in full scale plants. The differences in the chamber  
35 configuration (Desloover et al., 2011; Ren et al., 2013; Rodrigues Caballero et al., 2015; Hwang et  
36 al. 2016), chamber area and material (Aboobakar et al., 2013; Sun et al., 2015) and parameters  
37 monitored in the chamber (Pan et al., 2016; Rodriguez-Caballero et al., 2014), contribute to the  
38 complexity and to large variations in measurements of the key indicators of plant performance and

39 emissions (Cavazzuti, M. 2013). The full understanding of the uncertainties in GHG emissions and  
40 the biological processes in full scale wastewater systems is a pertaining challenge (Massara et al.,  
41 2017 and Daelman et al., 2015).

42 This study addresses this gap of knowledge by analysing the results of N<sub>2</sub>O emissions in a full-scale  
43 WWTP by performing classical (liquid chemical/physical characterization) and new data analytics  
44 techniques (online gaseous emissions and statistical analysis) to critically examine the relation  
45 between the monitored variables and N<sub>2</sub>O gaseous emissions. The study attempts both to calibrate  
46 the optimal sampling method and to systematically relate the gaseous emissions with the main liquid  
47 variables routinely analysed. Moreover, for the first time the critical role of the C:N ratio is discussed  
48 calculating the emission factors (EF) from the full-scale mass balances. Event-based sensitivity  
49 analysis (Tavakoli et al. 2013 a, b) is applied to identify potential dependencies between the system  
50 variables monitored online and the N<sub>2</sub>O emissions of the biological reactor.

## 51 **2. Material and methods**

### 52 **2.1 Wastewater treatment process**

53 The municipal wastewater treatment plant (WWTP) of Falconara Marittima (Italy) is fed by low C:N  
54 ratio wastewater. It has a design capacity of 80,000 PE and a design average influent flow of 30,000  
55 m<sup>3</sup>/d. Infiltration from groundwater and marine intrusions cause under-loading influent conditions  
56 during the dry weather. The real influent capacity (calculated on COD basis) is equal to 36,035±1,100  
57 PE during the period of this study. After degritting, desanding and primary settling, the wastewater  
58 is biologically treated with activated sludge process in two identical parallel lines applying the  
59 conventional Modified Ludzack Ettinger scheme. The total volume of the biological compartments  
60 is 13,700 m<sup>3</sup>. The aerated compartments are equipped by ceramic fine bubble diffusers; the air supply  
61 ranges between 1,870 and 9,210 m<sup>3</sup>/h. An automatic system controls the four blowers (Robuschi mod.

62 RBS LP120) based on the concentration of the dissolved oxygen (DO) in the aerobic reactor (three  
63 different operating settings: 0.4, 1.0 and 3.0 mg/L). The denitrification bioreaction volume is 8,860  
64 m<sup>3</sup>, with surface area of 507 m<sup>2</sup>. The nitrification bioreaction volume is 4,900 m<sup>3</sup>, with surface area  
65 of 560 m<sup>2</sup>. This study analyses one of the two parallel lines of the activated sludge bioreactor. The  
66 system is continuously monitored by on-line sensors (Dissolved Oxygen – DO- ; Temperature – T-;  
67 Mixed Liquor Suspended Solid-MLSS- and Oxidation Reduction Potential - ORP) and magnetic flow  
68 meters (influent, effluent, recirculation and waste sludge). The average sludge retention time (SRT)  
69 was 10 days and the sludge recycle ratio ( $Q_{\text{sludge recycled}}/Q_{\text{influent}}$ ) was 0.5. The MLVSS (Mixed Liquor  
70 Volatile Suspended Solids) concentration was 3,485±636 mg/L (ratio MLVSS/MLSS 0.61). The DO  
71 in the nitrification reactor was 4.3±0.9 mgO<sub>2</sub>/L and the pH was buffered at 8.1±0.2 due to under-  
72 loading characteristics of the influent. The monitoring campaign was lasted 52 days (September-  
73 November) with average temperature of 17.7±1.5 °C.

## 74 **2.2 Analytical methods and biomass activity tests**

75 Mixed-liquor grab samples were collected twice per week from the aerobic and pre-anoxic reactors,  
76 whereas 24h composite samples were taken twice per week from the influent and once per week from  
77 the effluent. All the samples were analysed in terms of pH, chemical oxygen demand (COD), total  
78 Kjeldahl nitrogen (TKN), ammonia nitrogen (NH<sub>4</sub>-N ), soluble COD (sCOD), nitrate nitrogen (NO<sub>3</sub>-  
79 N) and nitrite nitrogen (NO<sub>2</sub>-N) according to standard methods (APHA, 2005). The soluble COD was  
80 measured in the filtrate obtained after the filtration of the sample through Whatman 0.45 µm  
81 membrane filters. NO<sub>2</sub>-N, NO<sub>3</sub>-N were measured by ion chromatography in samples that were first  
82 filtered through 0.45 µm Whatman membranes (Dionex DX120).

83 Influent NH<sub>4</sub>-N was monitored in real-time (by AISE-Ammonium Probe- Hach Lange Ltd) for a  
84 relevant week in the influent to the activated sludge reactor. Moreover, influent samples were  
85 collected every 2 hours in a day to quantify the typical hourly of the C:N ratio. The mechanisms for

86 N<sub>2</sub>O production were not studied by additional dissolved N<sub>2</sub>O in the liquid phase because this  
87 knowledge has been provided by other bench- or pilot-scale studies (Mannina et al., 2018; Wunderlin  
88 et al., 2012). However, a significant gap of knowledge concerns the full scale WWTPs especially  
89 considering the real variable influent characteristics (i.e. C:N) and gaseous mass loads directly  
90 emitted in the atmosphere.

91 Moreover, to monitor the stability of the respiratory activity of the microbial community, nitrification  
92 and denitrification kinetics were analysed by batch tests. To determine the ammonia utilization  
93 rate AUR, 1.5 L of mixed liquor was collected from the aerobic reactor and was placed in a flask  
94 under continuous aeration (DO > 4 mg/L). After 30 min, the biomass was spiked with ammonium  
95 chloride at 40 mgNH<sub>4</sub>-N/L initial concentration and the profiles of ammonium, nitrite and nitrate with  
96 time were measured. All batch respirometry tests were conducted at room temperature (25 ± 2 °C)  
97 and the pH was maintained at 7.4 ± 0.3. The reported activities were normalized to the reference  
98 temperature of 20 °C using the Arrhenius temperature correction equation and to the volatile  
99 suspended solids (VSS) of the mixture. The nitrate utilization rate (NUR) tests were conducted with  
100 1.5 L of activated sludge placed in a flask, under mild agitation. Subsequently, the biomass was spiked  
101 with fixed nitrate concentration and with an external carbon source (acetic acid) and the nitrate  
102 profiles were measured.

### 103 **2.3 N<sub>2</sub>O sampling and monitoring strategies**

104 N<sub>2</sub>O emissions were continuously monitored with MIR9000CLD analyser (Environment Italia  
105 S.p.A.). The analyser measures N<sub>2</sub>O, CO<sub>2</sub> and CH<sub>4</sub> through infrared spectroscopy (IRS) and the NO  
106 and NO<sub>2</sub> by chemiluminescence (Eusebi et al., 2016). Weekly calibration using standard gas cylinders  
107 was performed. The gas flow was pumped, transported by a heating tube at 120°C, filtered for dust  
108 removal and cooled at 4°C. More than one type of sampling chamber was tested to optimize the N<sub>2</sub>O  
109 measurement procedure. In particular, two different types of gas chambers were used: fixed and

110 floating. The main characteristics of the different gas chambers are shown in Table 1 and in Table 2  
111 as 3D images, shapes, volumes and configurations. An open tube is located on the surface to allow  
112 gas suction. The outlet pipe was the same for the different gas hoods (diameter of 10 cm and length  
113 of 1 m).

114 Table 1

115 Table 2

116 The sampling point to measure the N<sub>2</sub>O emissions was chosen in the aerobic reactor as basin where  
117 the gaseous products were mainly stripped and emitted in the atmosphere. The sampling point was  
118 placed at the head of the reactor in the aerobic basin for 46 days and at the end for 7 days. The fixed  
119 chambers were attached to the external wall by steel clamps and the floating chamber was fastened  
120 by ropes. The minimum monitoring duration for each gas hood was 7 days. High-density polyethylene  
121 (HDPE) was used for the fixed gas hoods and polypropylene (PP) was used for the floating hoods.  
122 The base of the fixed gas chambers was submersed (about 5 cm) to prevent lateral movement and  
123 introduction of external air. Cylindrical fixed chambers were used with volumes equal to 80 L, 141  
124 L and 226 L for the small, medium and large chamber. The floating gas chambers had a truncated  
125 cone structure and volumes equal to 64 L (small), 166 L (medium) and 233 L (big) (Table 2).

126 At the end of the continuous monitoring phase, the emission factors were calculated as emitted N<sub>2</sub>O  
127 mass load from the aerobic reactor and they were related to the total influent nitrogen load.

#### 128 **2.4 N<sub>2</sub>O emissions and gas chamber headspace: optimization of the sampling methodology**

129 Initial calibration tests (N° 36) were performed to optimize the sampling method. The main objective  
130 of the tests was to identify the best sampling methodology in terms of different types/dimensions of  
131 the applied chambers shown in Table 1 and Table 2. The tests were carried out during the first 15  
132 days of dry weather. The sampling point was set at the head of the reactor. The tests were performed

133 in the same relevant period (from hrs 9.30 to hrs 12:30). Each test was carried out acquiring the N<sub>2</sub>O  
134 data for 1 hour with one type of chamber. At the end of the acquisition time the connection of the  
135 tube of the gases analyser was quickly moved from one chamber to another (small, medium or large,  
136 both floating and fixed) and another test started. Before and after this few-minutes operating time,  
137 the stable conditions in the liquid phase were monitored and verified by the analysis of the main  
138 dissolved nitrogen and organic forms (NH<sub>4</sub>-N, NO<sub>3</sub>-N, NO<sub>2</sub>-N, CODs). Therefore, the liquid  
139 conditions during the different short tests were comparable.

140 The N<sub>2</sub>O data was linked with two variables: 1) the air supply and 2) the Sampler Ratio (SR).

141 This second coefficient was set and calculated for each test according to equation 1:

$$S \left( L/m^3/h \right) = \frac{V_t \quad H \quad S}{A \quad S} \quad \text{Equation 1}$$

Where:

Volume Head Space (L) changes for each type of sampling chamber

Air Supply (m<sup>3</sup>/h) = Inlet air flow to the aerobic reactor

142 For the same type of chamber, the SR values dynamically varied because of the change of the air  
143 supply in the main biological reactor. Thus, the optimal dimension of the sampling chamber compared  
144 to the inlet airflow was studied to avoid over-estimation of N<sub>2</sub>O concentrations and/or overpressure  
145 phenomena.

## 146 **2.5 Event based data processing and sensitivity analysis**

147 An un-biased event-based sensitivity analysis was carried out in order to investigate dependencies  
148 between the N<sub>2</sub>O emissions and the parameters that were routinely monitored in biological process  
149 (APHA, 2005; Tavakoli et al., 2013) along the periods monitored by the different gas chambers  
150 (EventiC; Danishvar et al, 2017). This technique enables the identification of patterns (strength of

151 relations) between the monitored variables (DO, blowers flow rate, MLSS,  $Q_{in}$ ) and gas fluxes ( $N_2O$ ).  
152 Tangible and reasonable changes to the signals of the sensors in the system were translated into  
153 events. In order to track events in a sensor signal the standard deviation of the signal fluctuation for  
154 all the time period is calculated. Several thresholds were tested (ranging from 5% - 35% of the  
155 standard deviations of the variables) and presented the results that maximize the Event-based  
156 sensitivity analysis coefficients. The thresholds consider as events the following changes in the  
157 variables: i)  $DO > 0.2$  mg/l (>15% of the standard deviation); ii)  $N_2O > 0.1$  kg/h (>5% of the standard  
158 deviation); iii)  $MLSS > 20$  (>5% of the standard deviation); iv)  $Q_{in} > 20$  m<sup>3</sup>/h (>5% of the standard  
159 deviation); v) Blowers flow-rate > 110 m<sup>3</sup>/h (>5% of the standard deviation). The event-base  
160 sensitivity analysis enables the identification of cause-effect relationship between the causes of state  
161 change in the system and the system response and therefore provides insight on which input variables  
162 (i.e. ammonia, DO) impact a specific output (i.e.  $N_2O$ ). The un-biased sensitivity analysis detects and  
163 defines the most relevant variables (many to one and many to many relationships) by implementing  
164 the algorithm in the data from the different groups the influential variables in a look-up table. A  
165 detailed description of the method can be found in the study of Danishvar et al. (2017).

### 166 **3. Results and discussion**

#### 167 **3.1 Wastewater characteristics and plant performances**

168 The main influent and effluent characteristics are shown in Table 3. The influent flow-rate is  
169  $14,210 \pm 4,652$  m<sup>3</sup>/d. The TN concentration in the influent is  $28.6 \pm 10.5$  mg/L, mainly as ammonium  
170 nitrogen ( $25.1 \pm 3.2$  mg/L). The average effluent mass loads were  $2.87 \pm 2.00$  and  $196.50 \pm 86.05$  kgN/d  
171 of  $NH_4-N$  and TN. The TN and COD removal efficiencies were  $40 \pm 20\%$  and  $59 \pm 13\%$  respectively  
172 (Table 3).

173 Table 3



174 The low TN removal efficiency is related with the low biodegradable carbon to nitrogen ratio that  
175 limits the denitrification process. On the other hand, complete nitrification was achieved.  
176 Additionally, the AUR was  $0.111 \pm 0.024$  kgNH<sub>4</sub>-N/kgMLVSS/d and the average denitrification rate  
177 was  $0.057 \pm 0.028$  kgNO<sub>x</sub>-N/kgMLVSS/d.

178

179

### 180 **3.2 N<sub>2</sub>O emissions and gas chamber headspace: optimization of the sampling methodology**

181 The N<sub>2</sub>O concentrations obtained during the calibration tests for the optimization of the sampling  
182 methodology are shown in Figure 1 for different air flows both for the fixed and for the floating gas  
183 chambers (Figure 1 -a Fixed and -b Floating ). A linear increase of the N<sub>2</sub>O concentrations at higher  
184 influent air flux has been found in other works (Ribeiro et al., 2017). In the current work this  
185 behaviour has been observed only for the floating chambers (Figure 1-b). Scattered distribution was  
186 found for the fixed chambers (Figure 1-a). No evident relation was found between the increment of  
187 the N<sub>2</sub>O concentrations and the dimension (Small-Medium-Large) of the chamber used for sampling  
188 both for floating and for fixed chambers. Differently, the Sampler Ratio (SR-L/m<sup>3</sup>/h) was calculated  
189 according to Equation 1. The results showed that the N<sub>2</sub>O concentrations are linked with the SR value  
190 (Figure 1-c and -d) especially for the fixed chambers (Figure 1-c).

191

Figure 1-a-b-c-d

192 During the tests with high aeration flow-rate (SR <0.05 L/m<sup>3</sup>/h) in the fixed gas hoods, incremental  
193 N<sub>2</sub>O emissions peak were recorded. This is potentially attributed to compression phenomena in the  
194 head space of the fixed chambers and abrupt changes of the liquid level in the reactor. Therefore,  
195 during the continuous monitoring, N<sub>2</sub>O values with SR lower than 0.05 L/m<sup>3</sup>/h are not considered for  
196 the assessment of the N<sub>2</sub>O emission factor. The floating chambers performed better and were not

197 influenced by the SR variations (Figure 1-d); the same floating avoids potential over pressure  
198 phenomena in the head-space.

### 199 **3.3 N<sub>2</sub>O emission profiles during continuous monitoring**

200 The N<sub>2</sub>O emissions rate at the head of the reactor varied from 66.82 to 4,174.37 mg/h with average  
201 load equal to  $31.99 \pm 24.33$  gN<sub>2</sub>O/d during the monitoring period (Figure 2). The N<sub>2</sub>O emission profile  
202 was not affected by temperature variations ( $18.2 \pm 0.8$  °C in wastewater).

203 Figure 2

204 The variability of the daily N<sub>2</sub>O emissions rate can be mainly attributed to the actually variable  
205 influent carbon to nitrogen ratios (COD:TN: 1.3 to 5.2) that was always low. The average N<sub>2</sub>O  
206 emission rate was equal to  $0.856 \pm 0.905$  gN<sub>2</sub>O/h when the COD:TN was about 3.2 (1<sup>st</sup>-20<sup>th</sup> days),  
207 while it increased to  $1.850 \pm 0.972$  gN<sub>2</sub>O/h at lower COD:TN ratio:1.9. The latter is in accordance to  
208 the results reported in literature (Quan et al., 2012; Mannina et al., 2017). Similar limiting C:N ratios  
209 resulted in N<sub>2</sub>O increase in previous studies applying different processes (aerobic granular sludge  
210 sequencing batch reactors; integrated fixed film activated sludge membrane bioreactor, respectively)  
211 at pilot scale. Mannina et al. (2018) demonstrated that limiting C:N ratio of 2 gCOD/gTN resulted in  
212 5 times increase of N<sub>2</sub>O emissions from 0.12% to 5% (expressed as emitted N<sub>2</sub>O compared with the  
213 influent TN). Furthermore, in an Anammox process, C:N ratios of 3.0–0.65 were responsible for the  
214 increment of N<sub>2</sub>O production (Zhang et al., 2015).

215 Daelman et al. (Daelman et al., 2015) reported that the N<sub>2</sub>O emissions during the continuous  
216 monitoring were very low ( $0.174 \pm 0.90$  gN<sub>2</sub>O/h) at the end of the reactor. The geometry of the reactor  
217 was considered even in this study. The aerated activated sludge basin (length 35 and width 15 m) can  
218 be assimilated to n.3 completely stirred tank reactors that can lead to secondary behaviours observed  
219 in plug-flow configuration (Ming, 2016).

220 Moreover, the N<sub>2</sub>O emissions, the main operative variables and the daily variations were statistically  
221 analysed to better understand the role of the liquid variables. The boxplots of the hourly N<sub>2</sub>O  
222 emissions in the nitrification reactor are shown in Figure 3. N<sub>2</sub>O emissions' dynamics are  
223 characterized by significant daily variability in accordance with the results of previous studies  
224 (Aboobakar et al, 2013; Daelman et al., 2013; Rodriguez-Caballero et al., 2014).

225 Figure 3

226 The minimum daily N<sub>2</sub>O fluxes are observed between 03:00 am and 10:00 am, while a subsequent  
227 peak occurs between 18:00 pm and 20:00 pm. No specific correlation between the N<sub>2</sub>O emissions  
228 and the liquid influent flowrate was observed (Figure 3). Similar flow (about 500 m<sup>3</sup>/h) was recorded  
229 after hours 11:00 am without clear relation between the hydraulic overloading conditions and the  
230 peaks of N<sub>2</sub>O emissions.

231 Therefore, further analysis was undertaken by studying the hourly influent ammonia and COD  
232 concentrations. A typical example of daily variability is shown in Figure 4. Hourly variations between  
233 17.5 and 19.4 mg/L for ammonia nitrogen and between 61.6 and 20.1 mg/L for COD were observed  
234 with peaks of COD:TN during 12:00-16:00, where the N<sub>2</sub>O distribution showed almost minimum  
235 N<sub>2</sub>O emissions. The latter reveals that the variation of the COD:TN ratio strongly affects the N<sub>2</sub>O  
236 emissions during the day.

237 Figure 4

238 The cumulative emitted N<sub>2</sub>O mass loads (LN<sub>2</sub>O) and the influent TN (LTN) values are shown in  
239 Figure 5. The emission factors were reported for the periods characterized by COD:N lower than 4  
240 (1<sup>st</sup>-20<sup>th</sup> days), COD:N higher than 4 (21<sup>st</sup>-45<sup>th</sup> days) and when the sampling was carried out at the  
241 end of the reactor (Figure 5). The average N<sub>2</sub>O emission factor is 0.001 and 0.005 % of TN in the  
242 influent, respectively for the first (1<sup>st</sup>-20<sup>th</sup> days) and for the second period (21<sup>st</sup>-45<sup>th</sup> days). Lower

243 emissions are observed when the influent COD:N ratio is higher than 4. The lower was the COD:N  
244 ratio the higher was the emitted N<sub>2</sub>O: about 5 times higher compared to the periods with higher  
245 COD:TN ratio (0.0505 gN<sub>2</sub>O/kgTN, R<sup>2</sup>=0.8853).

246 **Figure 5**

247 The biomass-based EF was equal to 2.11±0.98 and 5.01±2.09 mgN<sub>2</sub>O/kgMLVSS/d for the first and  
248 second period with different COD:N ratios. The EF of current study is lower than the EF values  
249 reported in other studies that monitor on-line gaseous emissions at full-scale. Yan et al., 2014, found  
250 emission factors ranging from 0.04 to 0.1% of the TN influent for an Anaerobic-Anoxic-Oxic system.  
251 Similarly, Rodriguez-Caballero et al., 2014, reported N<sub>2</sub>O emissions equal to 0.116% of the influent  
252 TN in a plug-flow reactor.

### 253 **3.2 Statistical and sensitivity analysis**

254 An-event based sensitivity analysis was carried out in order to identify the relationship between the  
255 N<sub>2</sub>O emissions and the monitored parameters. The results are given Table 4. The gaseous emissions  
256 from the nitrification reactor have been examined with reference to the variables monitored online  
257 when the floating hood was applied with SR higher than 0.05 L/m<sup>3</sup>/h.

258 **Table 4**

259 A weak relationship was identified between the N<sub>2</sub>O emissions, the air flow-rate and the DO  
260 concentration in the reactor. In line with the results of this study, Rodriguez-Caballero et al. (2014)  
261 found that the N<sub>2</sub>O dynamics were not significantly affected by DO variations (within the range of  
262 1.5 – 2 mg/L) when the nitrification efficiency was constant. Moderate relationship was identified  
263 between the influent flow-rate and the N<sub>2</sub>O fluxes; the latter is supported by the daily behaviour of  
264 N<sub>2</sub>O emissions (Figure 3). Additionally, the MLSS concentration was relatively steady during the  
265 monitoring campaign and therefore, it is not directly linked with the behaviour of N<sub>2</sub>O emissions.

266 According to event-based sensitivity analysis, the blowers' flow-rate affects the N<sub>2</sub>O emission fluxes.  
267 The typical N<sub>2</sub>O emissions (g/h) profile is shown in Figure 6 with the aeration flow-rate and with the  
268 residual DO for two days of monitoring. Low concentrations of residual dissolved oxygen was not a  
269 limiting factor (Figure 6). The latter supports the obtained results during the experimental campaign  
270 considering the low impact of the DO concentrations (4.6±0.7 mg DO /l during 1<sup>st</sup>-20<sup>th</sup> days and  
271 4.1±1.6 mgDO/l during 21<sup>st</sup>-45<sup>th</sup> days) and the constant nitrification rates (kn of 0.116±0.016 kgNH<sub>4</sub>-  
272 N/kgMLVSS/d during 1<sup>st</sup>-20<sup>th</sup> days and kn of 0.118±0.031 kgNH<sub>4</sub>-N/kgMLVSS/d during 21<sup>st</sup>-45<sup>th</sup>  
273 days 4.1±1.6 mg/l).

274 Figure 6

275 The dynamics of the variables are different. However, daily peaks of N<sub>2</sub>O emissions occurred when  
276 the aeration flow-rate was higher than 3,500 m<sup>3</sup>/h. Therefore, although higher N<sub>2</sub>O emissions were  
277 related to the low C:N ratios that limited heterotrophic denitrification, higher aeration flow rates  
278 increase N<sub>2</sub>O stripping phenomena and related N<sub>2</sub>O emissions.

#### 279 **4 Conclusions**

280 A full scale activated sludge plant treating low carbon:nitrogen ratio municipal wastewater was  
281 continuously analysed for 52 days to study N<sub>2</sub>O emissions.

282 This long-term continuous critical monitoring led to the following conclusions related to: a) the  
283 sampling methods; b) the full scale observed effects of influent and operating variables. In particular:

284 a) the optimization of the sampling methods was carried out by testing different types of chambers.  
285 Uncertainties of the N<sub>2</sub>O concentrations were observed when the Sampling Ratio between the  
286 chamber volume and the air supply was lower than 0.05 L/m<sup>3</sup>/h. Finally, the floating chambers were  
287 more reliable compared to the fixed sampling systems.

288 b) the N<sub>2</sub>O load emitted directly from the aeration basin was related to the carbon to nitrogen ratio  
289 mainly and to the variability of the influent load. Low COD:N ratio limited the denitrification and led  
290 to 5-times higher N<sub>2</sub>O emissions. Major differences were observed around the COD:TN = 4:  
291 0.856±0.905 gN<sub>2</sub>O/h when COD:TN > 4 versus 1.850±0.972 gN<sub>2</sub>O/h when COD:TN < 4. The  
292 statistical elaboration of N<sub>2</sub>O emissions further supported those conclusions: hourly N<sub>2</sub>O peak  
293 emissions are higher when the COD:N ratio is lower. The sensitivity analysis showed that the N<sub>2</sub>O  
294 dynamics are not significantly affected by DO variations (within the range of 1.5 – 2 mg/L). However,  
295 daily peaks of N<sub>2</sub>O emissions are observed at higher aeration flow-rate that result in higher stripping  
296 of the produced and dissolved N<sub>2</sub>O.

297 Finally, when COD:N ratio was higher than 4, the cumulative emitted N<sub>2</sub>O mass loads (EF) varied  
298 from 0.051 gN<sub>2</sub>O/kgTN<sub>influent</sub> to 0.0089 gN<sub>2</sub>O/kgTN<sub>influent</sub>. Therefore, the equalization of the influent  
299 can be advantageous even in terms of N<sub>2</sub>O emissions.

### 300 **Acknowledgements**

301 This study was supported by the Horizon 2020 research and innovation programme, within the  
302 SMART-Plant Innovation Action (grant agreement No 690323). The authors would like to  
303 acknowledge the Royal Society for the funding of the current research: Ad-Bio, Advanced  
304 Fellowship-2015/R2. The authors gratefully acknowledge the local water utility Multiservizi S.p.A.  
305 for its availability and practical support during the tests in the WWTP of Falconara Marittima  
306 (Ancona, Italy).

307

308

309

310 **References**

- 311 Aboobakar, A. Cartmell, E. Stephenson, T. Jones, M. Vale, P. Dotro, G. (2013) Nitrous oxide  
312 emissions and dissolved oxygen profiling in a full-scale nitrifying activated sludge treatment  
313 plant, *Water Research* 47 524–534. doi:10.1016/j.watres.2012.10.004.
- 314 APHA, 2005, Standard methods for the examination of water and wastewater, Am. Public Health  
315 Assoc. APHA Wash. DC USA. (2005).  
316 www.just.edu.jo/CoursesAndLabs/ENVIRONMENTAL%20ANALYTICAL%20CHEMISTRY  
317 \_CHEM734/chem%20734.doc. Last access September 2017.
- 318 Bollon, J. Filali, A. Fayolle, Y. Guerin, S. Rocher, V. Gillot, S. (2016) N<sub>2</sub>O emissions from full-scale  
319 nitrifying biofilters, *Water Research* 102 41–51. DOI:10.1016/j.watres.2016.05.091
- 320 Daelman, M.R. van Voorthuizen, E.M. van Dongen, U.G. Volcke, E.I. van Loosdrecht, M.C. (2015)  
321 Seasonal and diurnal variability of N<sub>2</sub>O emissions from a full-scale municipal wastewater  
322 treatment plant, *Science Total Environment* 536 1–11.  
323 <https://doi.org/10.1016/j.scitotenv.2015.06.122>
- 324 Daelman, M.R.J. van Voorthuizen, E.M. Van Dongen, L. Volcke, E.I.P. Van Loosdrecht, M.C.M.  
325 (2013) Methane and nitrous oxide emissions from municipal wastewater treatment—results from  
326 a long-term study, *Water Science Technology* 67 2350–2355. DOI:10.2166/wst.2013.109
- 327 Danishvar, M. Mousavi, A. Broomhead, P. (2017) Modelling the Eco-System of Causality: The Real-  
328 Time Unaware Event-Data Clustering (EventiC), accepted to *IEEE Trans Systems, Man and*  
329 *Cybernetics*.
- 330 Desloover, J. De Clippeleir, H. Boeckx, P. Du Laing, G. Colsen, J. Verstraete, W. Vlaeminck, S.E.  
331 (2011) Floc-based sequential partial nitrification and anammox at full scale with contrasting N<sub>2</sub>O

332 emissions, *Water Research* 45 2811–2821. doi:10.1016/j.watres.2011.02.028.  
333 <https://doi.org/10.1016/j.watres.2011.02.028>

334 Eusebi, A.L., Cingolani, D., Spinelli, M, Passserini, G., Carletti, S., Battistoni, P. (2016) Dinitrogen  
335 oxide (N<sub>2</sub>O) emission in the treatment of urban wastewater via nitrite: Influence of liquid kinetic  
336 rates. *Water Science and Technology*, 74 (12), pp. 2784-2794 DOI: 10.2166/wst.2016.445

337 Guanghuan Ge, Jianqiang Zhao, Xiaoling Li, Xiaoqian Ding, Aixia Chen, Ying Chen, Bo Hu, and  
338 Sha Wang, (2017) Effects of influent COD/N ratios on nitrous oxide emission in a sequencing  
339 biofilm batch reactor for simultaneous nitrogen and phosphorus removal. *Scientific Report* 2017;  
340 7: 7417 doi: 10.1038/s41598-017-06943-0

341 He, Q., Zhu, Y., Fan, L., Ai, H., Huangfu, X., Chen, M. (2017) Effects of C/N ratio on nitrous oxide  
342 production from nitrification in a laboratory-scale biological aerated filter reactor. *Water Science  
343 and Technology*, 75, (6), pp1270-1280 DOI: 10.2166/wst.2016.447

344 Hwang, K.-L. Bang, C.-H. Zoh, K.-D. (2016) Characteristics of methane and nitrous oxide emissions  
345 from the wastewater treatment plant, *Bioresource Technology* 214 881–884.  
346 doi:10.1016/j.biortech.2016.05.047. DOI:10.1016/j.biortech.2016.05.047

347 IPCC, The physical science basis. Contribution of working group I to the fifth assessment report of  
348 the intergovernmental panel on climate change, USA: Cambridge University Press, 2013.

349 Kampschreur, M.J. van der Star, W.R. Wiolders H.A., Mulder, J.W. Jetten, M.S. van Loosdrecht,  
350 M.C. (2008) Dynamics of nitric oxide and nitrous oxide emission during full-scale reject water  
351 treatment, *Water Research* 42 812–826. <https://doi.org/10.1016/j.watres.2007.08.022>



352 Law, Ye, Pan, Yuan, (2012), Low Nitrous oxide emissions from wastewater treatment processes.  
353 Philosophical Transactions of the Royal Society B 2012 May 5; 367(1593): 1265–1277.  
354 DOI:10.1098/rstb.2011.0317

355 Mannina, Capodici, Cosenza, Di Trapani M.C.van Loosdrecht (2017) Nitrous oxide emission in a  
356 University of Cape Town membrane bioreactor: The effect of carbon to nitrogen ratio. Journal of  
357 Cleaner Production. Volume 149, Pages 180-190. doi.org/10.1016/j.jclepro.2017.02.089

358 Mannina, Ekama, Capodici, Cosenza, Di Trapani, Ødegaard, M.C.van Loosdrecht, (2018) Influence  
359 of carbon to nitrogen ratio on nitrous oxide emission in an Integrated Fixed Film Activated Sludge  
360 Membrane BioReactor plant, Journal of Cleaner Production Volume 176, Pages 1078-1090  
361 doi.org/10.1016/j.jclepro.2017.11.222

362 Mannina, G., Capodici, M., Cosenza, A., Di Trapani, D. (2018) Nitrous oxide from integrated fixed-  
363 film activated sludge membrane bioreactor: Assessing the influence of operational variables.  
364 Bioresource Technology Volume 247, January 2018, Pages 1221-1227  
365 doi.org/10.1016/j.biortech.2017.09.083

366 Massara, T.M. Malamis, S. Guisasola, A. Baeza, J.A. Noutsopoulos, C. Katsou, E. (2017) A review  
367 on nitrous oxide (N<sub>2</sub>O) emissions during biological nutrient removal from municipal wastewater  
368 and sludge reject water, Science Total Environment 596 106–123. DOI:  
369 10.1016/j.scitotenv.2017.03.191

370 Ming, Glasser, Hildebrandt, Glasser, Metzger Fundamental Reactor Type, First published: 23  
371 September 2016 Wiley Online Library

372 Mingming Gao, Sen Yang, Mingyu Wang, Xin-Hua Wang, (2016), Nitrous oxide emissions from an  
373 aerobic granular sludge system treating low-strength ammonium wastewater. Journal of

374 Bioscience and Bioengineering Volume 122, 5, 601-605  
375 <https://doi.org/10.1016/j.jbiosc.2016.04.004>

376 Pan, Y. van den Akker, B. Ye, L. Ni, B.-J. Watts, S. Reid, K. Yuan, Z. (2016) Unravelling the spatial  
377 variation of nitrous oxide emissions from a step-feed plug-flow full scale wastewater treatment  
378 plant, Scientific Report 6. doi:10.1038/srep20792.

379 Quan, X. Zhang, M. Lawlor, P.G. Yang, Z. Zhan, X. (2012) Nitrous oxide emission and nutrient  
380 removal in aerobic granular sludge sequencing batch reactors, Water Research 46 4981–4990.  
381 <https://doi.org/10.1016/j.watres.2012.06.031>

382 Ren, Y. g. Wang, J. h. Li, H. f. Zhang, J. Qi, P. y. Hu, Z. (2013) Nitrous oxide and methane emissions  
383 from different treatment processes in full-scale municipal wastewater treatment plants,  
384 Environmental Technology 34 2917–2927. doi:10.1080/09593330.2012.696717.

385 Ribeiro P., Renato F. Bueno, Rodrigo P. Piveli, C. Kligerman, Roque Débora, de Mello, William Z.  
386 Oliveira Jaime L. M., (2017), The response of nitrous oxide emissions to different operating  
387 conditions in activated sludge wastewater treatment plants in Southeastern Brazil. Water Science  
388 Technology, 76, 3. DOI: 10.2166/wst.2017.399

389 Rodriguez-Caballero, A. Aymerich, I. Marques, R. Poch, M. Pijuan, M. (2015) Minimizing N<sub>2</sub>O  
390 emissions and carbon footprint on a full-scale activated sludge sequencing batch reactor, Water  
391 Research 71 1–10. doi:10.1016/j.watres.2014.12.032.

392 Rodriguez-Caballero, A. Aymerich, I. Poch, M. Pijuan, M. (2014) Evaluation of process conditions  
393 triggering emissions of green-house gases from a biological wastewater treatment system, Science  
394 Total Environment 493 384–391. doi:10.1016/j.scitotenv.2014.06.015.

395 Sun, S. Bao, Z. Sun, D. (2015) Study on emission characteristics and reduction strategy of nitrous  
396 oxide during wastewater treatment by different processes, *Environmental Science Pollution*  
397 *Research* 22 4222–4229. doi:10.1007/s11356-014-3654-5.

398 Tavakoli, S. Mousavi, A. Broomhead, P. (2013) Event tracking for real-time unaware sensitivity  
399 analysis (EventTracker), *IEEE Transaction Knowledge Data Engineering* 25 348–359. DOI:  
400 10.1109/TKDE.2011.240

401 Tavakoli, S. Mousavi, A. Poslad, S. (2013) Input variable selection in time-critical knowledge  
402 integration applications: A review, analysis, and recommendation paper, *Advanced Engineering*  
403 *Information* 27 519–536. <https://doi.org/10.1016/j.aei.2013.06.002>

404 Wunderlin, P. Mohn, J. Joss, A. Emmenegger, L. Siegrist H. (2012), Mechanisms of N<sub>2</sub>O production  
405 in biological wastewater treatment under nitrifying and denitrifying conditions *Water Research*,  
406 46 (4) pp. 1027-1037 doi.org/10.1016/j.watres.2011.11.080

407 Yan, X. Li, L. Liu, J. (2014) Characteristics of greenhouse gas emission in three full-scale wastewater  
408 treatment processes, *Journal Environmental Science* 26 256–263. [https://doi.org/10.1016/S1001-](https://doi.org/10.1016/S1001-0742(13)60429-5)  
409 [0742\(13\)60429-5](https://doi.org/10.1016/S1001-0742(13)60429-5)

410 Zhang Y, Ji G, Wang R. (2016) Drivers of nitrous oxide accumulation in denitrification biofilters  
411 with low carbon:nitrogen ratios. *Water Research* 2016 Dec 1;106:79-85. DOI:  
412 10.1016/j.watres.2016.09.046

413 Zheng, M. Tian, Y. Liu, T. Ma, T. Li, L. Li, C. Ahmad, M. Chen, Q. Ni, J. (2015) Minimization of  
414 nitrous oxide emission in a pilot-scale oxidation ditch: Generation, spatial variation and microbial  
415 interpretation, *Bioresource Technology* 179 510–517. doi.org/10.1016/j.biortech.2014.12.027

416

417 **List of Tables**

418 **Table 1:** Characteristics of the sampling gas chambers

419 **Table 2.** 3D Images, shapes and volumes of the sampling gas chambers

420 **Table 3:** Daily influent and effluent characteristics and kinetic rates (Average and Standard  
421 Deviation)

422 **Table 4:** Event-based sensitivity analysis algorithm grouping the system parameters in which events  
423 have systematically coincided (dark grey: high impact, light grey: moderate impact)

424

425

426

427

428

429

430

431

432

433

434

435

436

437

**Table 1:** Characteristics of the sampling gas chambers

Type	Shape	Size	Surface (m <sup>2</sup> )	Min	Max	Average	Std. Dev
Fixed	Cylinder	Small	0.157	0.086	0.100	0.095	0.005
		Medium	0.174	0.130	0.238	0.184	0.045
		Large	0.246	0.210	0.289	0.251	0.035

---

Floating	Truncated Cone	Small	0.125	0.101	0.185	0.139	0.032
		Medium	0.325	0.090	0.130	0.106	0.011
		Large	0.457	0.097	0.105	0.102	0.003

---

438

439

440

441

442

443

444

445

446

447

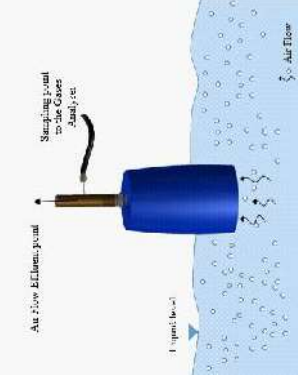
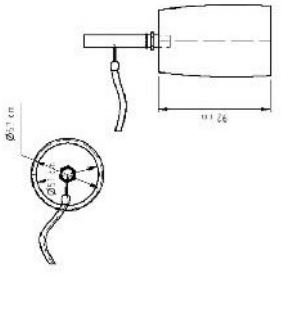
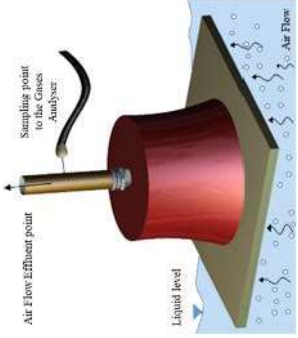
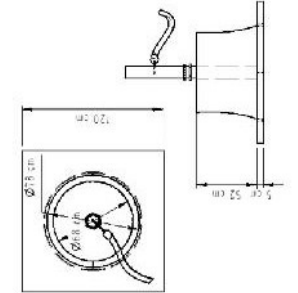
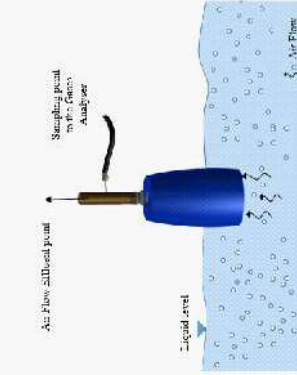
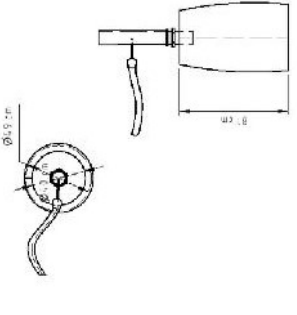
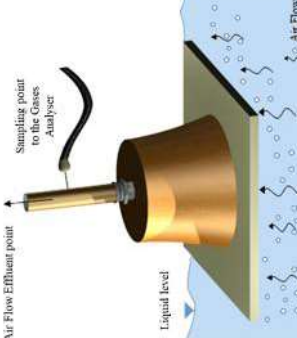
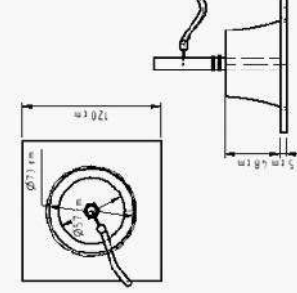

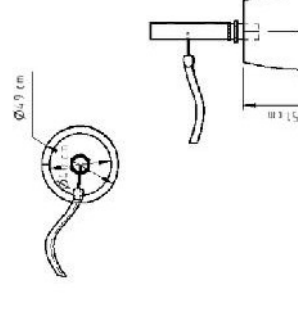
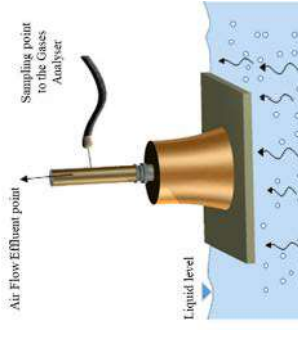
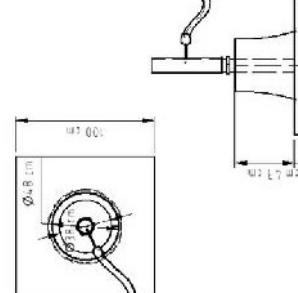
448

449

450

451

Table 2: 3D Images, shapes and volumes of the sampling gas chambers

Sampler with Fixed Chamber		Sampler with Floating Chamber	
3D Image	Specific Dimensions	3D Image	Specific Dimensions
Large	Useful Volume ~ 230 L	Large	Useful Volume ~ 230 L
			
Medium	Useful Volume ~ 150 L	Medium	Useful Volume ~ 150 L
			
Small	Useful Volume ~ 70 L	Small	Useful Volume ~ 70 L
			

**Table 3: Daily influent and effluent characteristics and kinetic rates (Average and Standard Deviation)**

	pH	TSS	COD	CODs	TKN	NH <sub>4</sub> -N	NO <sub>2</sub> -N	NO <sub>3</sub> -N	kn	kd <sub>max</sub>	Real kd
		mg/L	mg/L	mg/L	mg/L	mg/L	mg/L	mg/L	$\frac{\text{kgNH}_4^+}{\text{N/kgMLVSS/d}}$	%	%
Influent	8.1 (±0.2)	36.8 (±15.0)	88.7 (±33.5)	41.6 (±20.5)	28.6 (±10.5)	25.1 (±3.2)	0.3 (±0.2)	0.9 (±0.8)	0.111 (±0.024)	0.057 (±0.028)	0.017 (±0.005)
Effluent	7.9 (±0.1)	5.1 (±2.4)	35.1 (±5.5)	-	14.5 (±5.3)	0.2 (±0.2)	0.0 (±0.0)	12.0 (±4.6)	-	-	-
Efficiency (%)	-	-	59 (±13)	-	40 (±20)	99 (±1)	-	-	-	-	-

**Table 4:** Event-based sensitivity analysis algorithm grouping the system parameters in which events have systematically coincided (dark grey: high impact, light grey: moderate impact).

	N <sub>2</sub> O (ppm)
Q <sub>in</sub> (m <sup>3</sup> /h)	0.52
DO (mg/L)	0.37
Blowers flow-rate (m <sup>3</sup> /h)	0.44
MLSS	0.39



## List of Figures

**Figure 1:** N<sub>2</sub>O emissions during the tests for the calibration of the sampling chambers

**Figure 2:** N<sub>2</sub>O emissions in nitrification reactor

**Figure 3:** Boxplots of the daily variability of N<sub>2</sub>O emissions and Influent Flow (grey boxes: interquartile range, whiskers: lines extending from the 5<sup>th</sup> to 95<sup>th</sup> percentile, median: line across the box; grey triangles: average liquid influent flow rate)

**Figure 4:** Daily variability of NH<sub>4</sub>-N and COD concentrations in the influent liquid flow

**Figure 5:** Cumulative mass load of N<sub>2</sub>O emitted and TN influent (Averages and Standard Deviations).

**Figure 6:** Profile of the N<sub>2</sub>O emissions, air flow-rate and DO data for the nitrification reactor

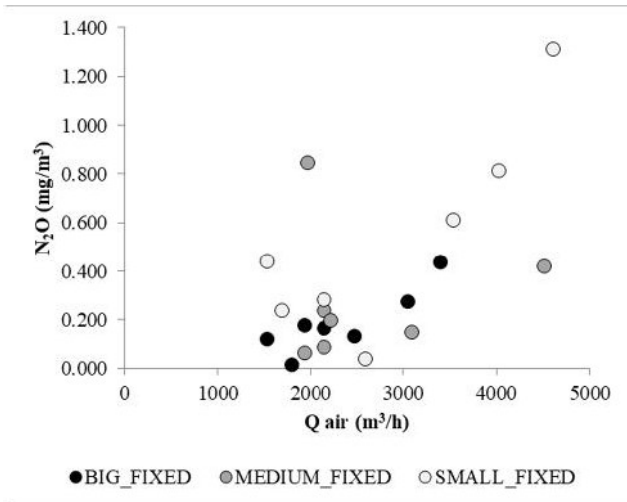


Figure 1 a- N<sub>2</sub>O-inlet air flow-Fixed gas chambers

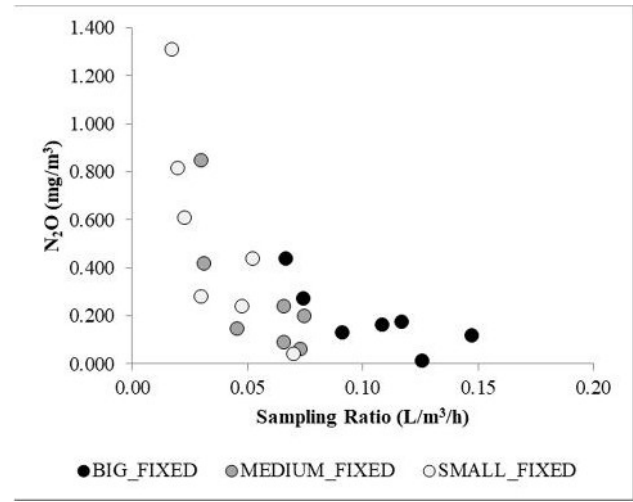


Figure 1 b- N<sub>2</sub>O-inlet air flow-Floating gas chambers

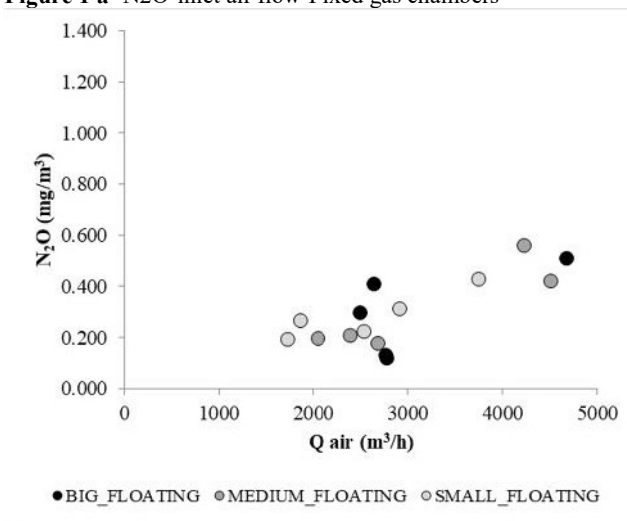


Figure 1 c- N<sub>2</sub>O emission/SR-Fixed gas chambers

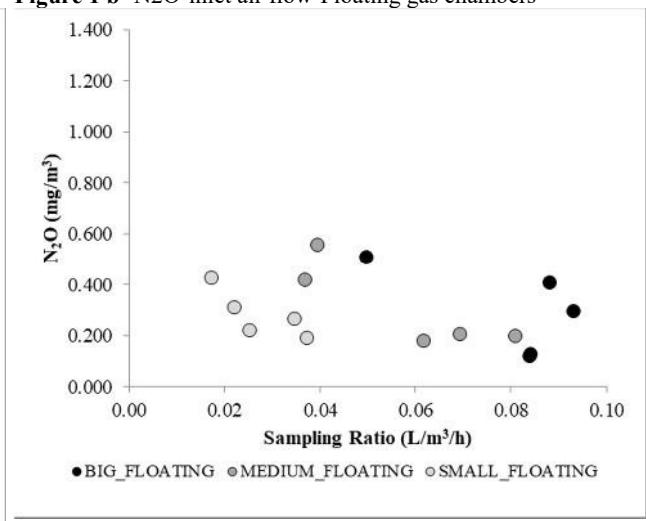
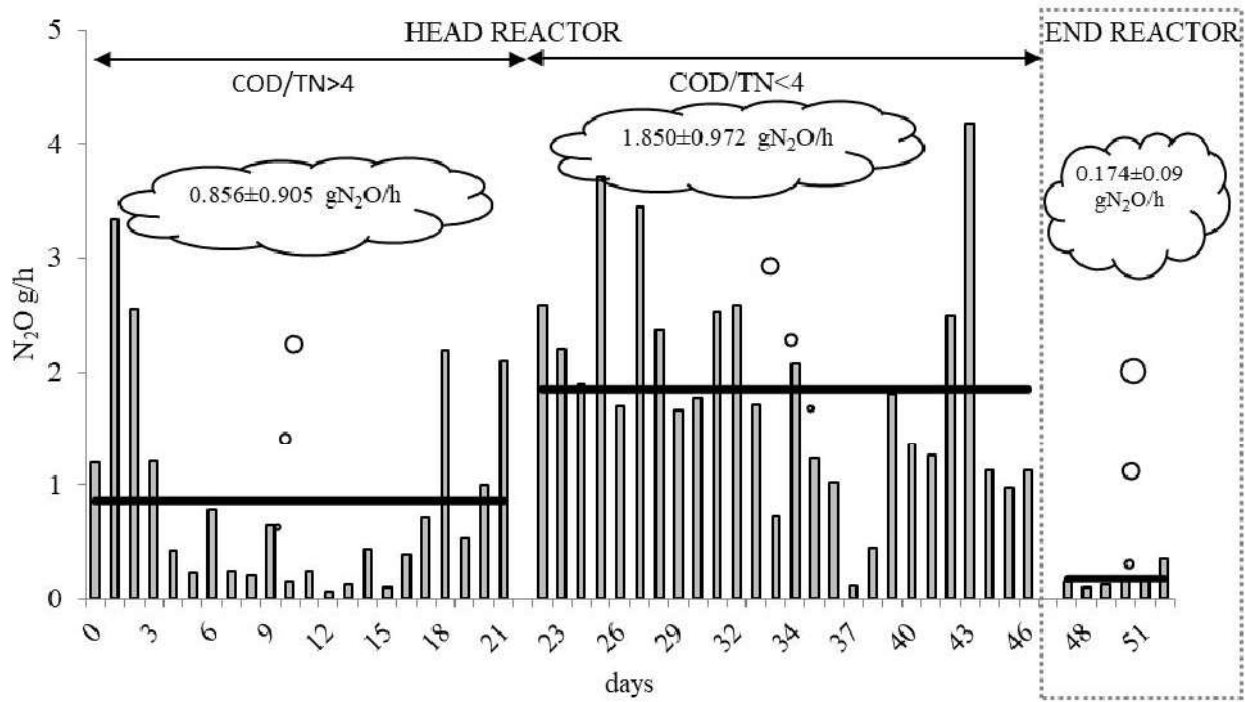
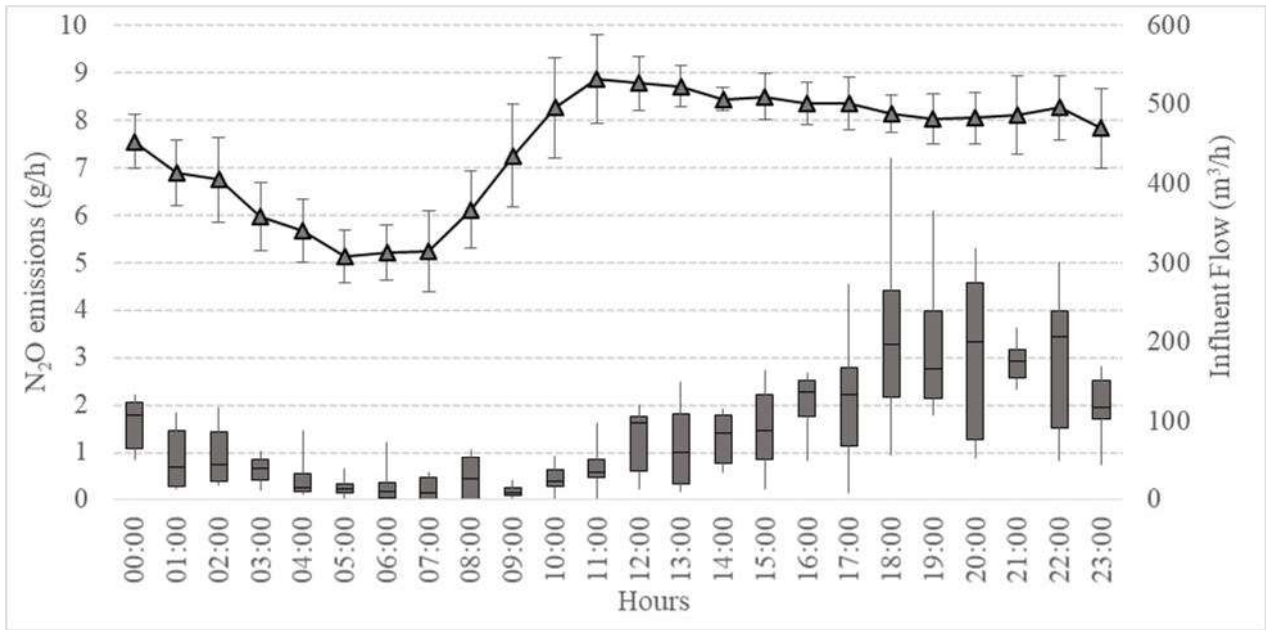


Figure 1 d- N<sub>2</sub>O emission/SR-Floating gas chambers

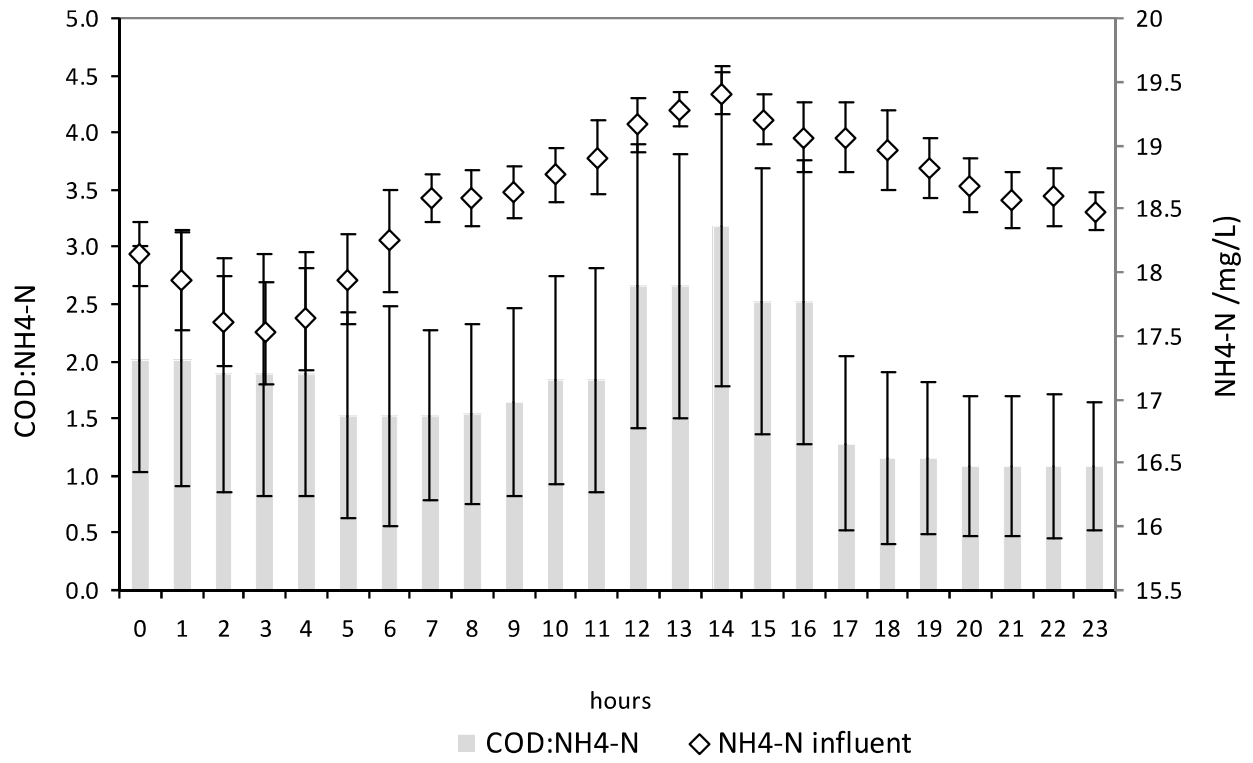
Figure 1: N<sub>2</sub>O emissions during the tests for the calibration of the sampling chambers



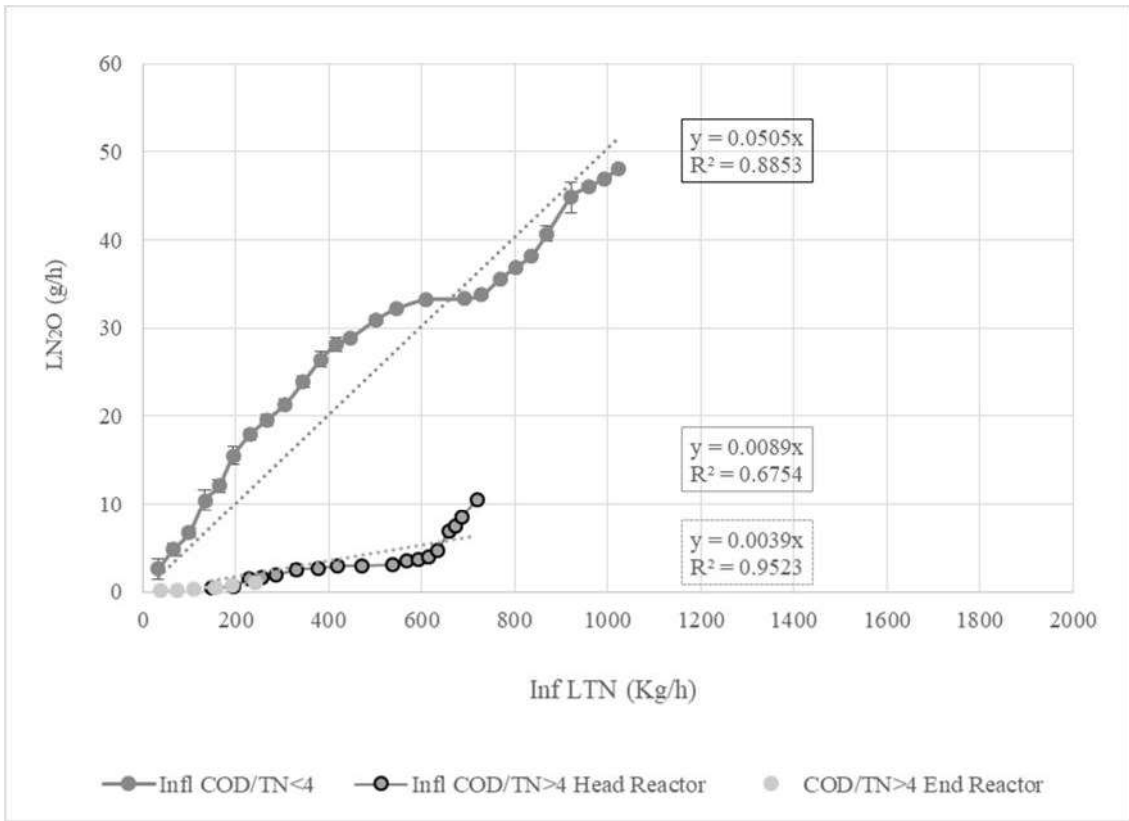
**Figure 2:** N<sub>2</sub>O emissions in nitrification reactor



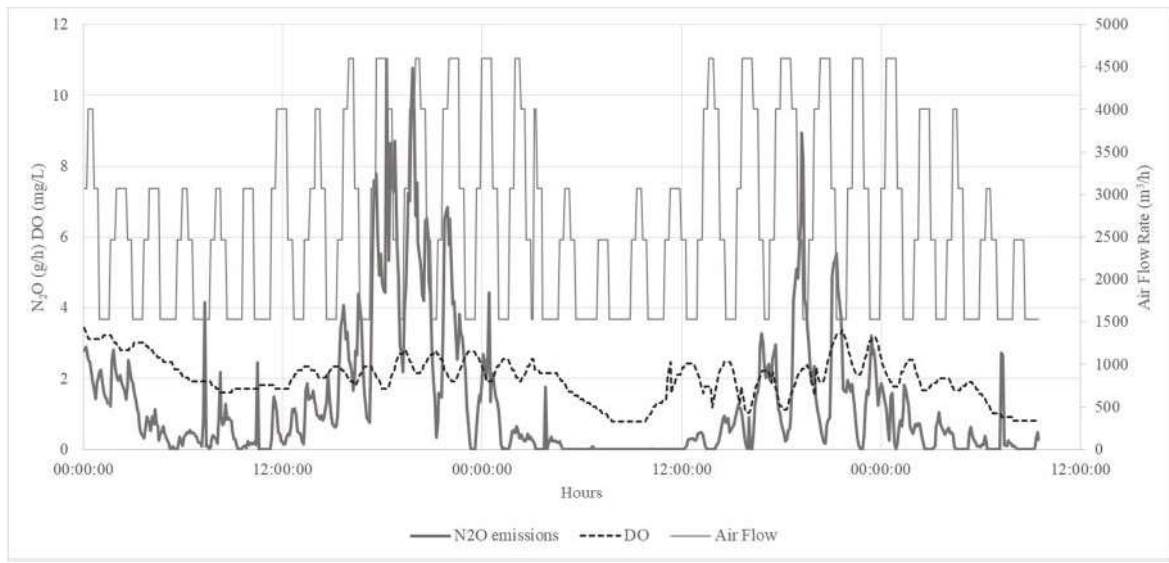
**Figure 3:** Boxplots of the daily variability of N<sub>2</sub>O emissions and Influent Flow (grey boxes: interquartile range, whiskers: lines extending from the 5th to 95th percentile, median: line across the box; grey triangles: average liquid influent flow rate)



**Figure 4:** Typical daily variability of COD/NH<sub>4</sub>-N and NH<sub>4</sub>-N concentrations in the influent liquid flow



**Figure 5:** Cumulative mass load of N<sub>2</sub>O emitted and TN influent (Averages and Standard Deviations).



**Figure 6:** Profile of the N<sub>2</sub>O emissions, air flow-rate and DO data for the nitrification reactor